

# Molecular characterization of three novel splicing mutations causing factor V deficiency and analysis of the *F5* gene splicing pattern

Claudia Dall'Osso,<sup>1</sup> Ilaria Guella,<sup>1</sup> Stefano Duga,<sup>1</sup> Nadia Locatelli,<sup>1</sup> Elvezia Maria Paraboschi,<sup>1</sup> Marta Spreafico,<sup>2</sup> Abdolreza Afrasiabi,<sup>3</sup> Christoph Pechlaner,<sup>4</sup> Flora Peyvandi,<sup>2</sup> Maria Luisa Tenchini,<sup>1</sup> and Rosanna Asselta<sup>1</sup>

<sup>1</sup>Department of Biology and Genetics for Medical Sciences, University of Milan, Italy; <sup>2</sup>A. Bianchi Bonomi, Hemophilia and Thrombosis Center, University of Milan and Department of Medicine and Medical Specialties, IRCCS Maggiore Hospital, Mangiagalli and Regina Elena Foundation, Milan, Italy; <sup>3</sup>Hemostasis and Thrombosis Unit, Haematology Research Center, Shiraz Medical University of Science, Shiraz, Iran and <sup>4</sup>Innsbruck Medical University, University Hospital, Department of Internal Medicine, Innsbruck, Austria

## ABSTRACT

### Background

Factor V deficiency is a rare autosomal recessive hemorrhagic disorder, associated with bleeding manifestations of variable severity. In the present study, we investigated the molecular basis of factor V deficiency in three patients, and performed a comprehensive analysis of the factor V gene (*F5*) splicing pattern.

### Design and Methods

Mutational screening was performed by DNA sequencing. Wild-type and mutant *F5* mRNA were expressed by transient transfection in COS-1 cells, followed by reverse-transcriptase polymerase chain reaction and sequencing. Real-time reverse-transcriptase polymerase chain reaction was used to evaluate degradation of mRNA carrying premature termination codons.

### Results

Mutational screening identified three hitherto unknown splicing mutations (IVS8+6T>C, IVS21+1G>A, and IVS24+1\_+4delGTAG). Production of mutant transcripts in COS-1 cells demonstrated that both IVS21+1G>A and IVS24+1\_+4delGTAG cause the activation of cryptic donor splice sites, whereas IVS8+6T>C causes exon-8 skipping (*F5*- $\Delta$ 8-mRNA). Interestingly, *F5*- $\Delta$ 8-mRNA was also detected in wild-type transfected samples, human liver, platelets, and HepG2 cells, demonstrating that *F5* exon-8 skipping takes place physiologically. Since *F5*- $\Delta$ 8-mRNA bears a premature termination codons, we investigated whether this transcript is subjected to nonsense-mediated mRNA decay degradation. The results confirmed the involvement of nonsense-mediated mRNA decay in the degradation of *F5* PTC<sup>+</sup> mRNA. Moreover, a comprehensive analysis of the *F5* splicing pattern led to the identification of two in-frame splicing variants resulting from skipping of exons 3 and 5-6.

### Conclusions

The functional consequences of three splicing mutations leading to FV deficiency were elucidated. Furthermore, we report the identification of three alternatively spliced *F5* transcripts.

Key words: factor V deficiency, *F5*, splicing mutations, nonsense-mediated mRNA decay, exon skipping, premature termination codons.

Citation: Dall'Osso C, Guella I, Duga S, Locatelli N, Paraboschi EM, Spreafico M, Afrasiabi A, Pechlaner C, Peyvandi F, Tenchini ML, and Asselta R. Molecular characterization of three novel splicing mutations causing factor V deficiency and analysis of the *F5* gene splicing pattern. *Haematologica* 2008; 93:1505-1513. doi: 10.3324/haematol.12934

©2008 Ferrata Storti Foundation. This is an open-access paper.

*Acknowledgments: the authors wish to thank Veronica Astro for excellent technical assistance, and Dr. G. Piseddu (Servizio di Coagulazione, Servizio di Prevenzione, Diagnosi e Terapia delle Malattie Emorragiche e Trombotica, Azienda USL n. 1, Sassari, Italy) for clinical identification of the probands, taking the family histories and collecting blood samples. We also thank all members of the families analyzed in this study for their participation.*

*Funding: RA is the recipient of a Bayer Hemophilia Early Career Investigator Award 2005. The financial support of PRIN (Programmi di Ricerca Scientifica di Rilevante Interesse Nazionale, Grant n. 2005058307\_002) and FIRCT (Fondo per gli Investimenti Ricerca Scientifica e Tecnologica) is gratefully acknowledged.*

*Manuscript received February 18, 2008. Revised version arrived June 6, 2008. Manuscript accepted June 11, 2008.*

*Correspondence: Rosanna Asselta, Ph.D., Department of Biology and Genetics for Medical Sciences, University of Milan, via Viotti 3/5, 20133 Milan, Italy. E-mail: rosanna.asselta@unimi.it*

## Introduction

Factor V (FV) deficiency (Mendelian Inheritance in Man +227400) is a rare inherited coagulation disorder, characterized by low or unmeasurable levels of FV antigen and coagulant activity.<sup>1</sup> This bleeding disorder has a prevalence of about one per million in the general population.<sup>2</sup> The clinical manifestations range from mild to severe<sup>3</sup> and include epistaxis, menorrhagia, easy bruising, and hemorrhages after trauma, surgery or dental extractions. Hemarthroses and hematomas occur in only one-quarter of the patients, and life-threatening bleeding episodes in the gastrointestinal tract and in the central nervous system are rare. Since no commercial FV concentrate is available, the treatment of this coagulation deficiency relies on the infusion of fresh-frozen plasma.<sup>2</sup>

The gene coding for human FV (*F5*) comprises 25 exons, covers a genomic region of 74.5 Kb and maps to chromosome 1q24.2 [UCSC Genome Browser, <http://genome.ucsc.edu/>].<sup>4</sup> Its 7-Kb open reading frame codes for a mature protein of 2196 amino acids.<sup>5</sup> To date, 42 genetic defects, all located in *F5*, have been reported as the cause of severe FV deficiency.<sup>1,6-11</sup> Among these, only four variations affecting splicing have so far been identified.<sup>10,12-14</sup>

It has been estimated that one-third of hereditary genetic diseases as well as many forms of cancer are caused by mutations resulting in the generation of transcripts bearing a premature termination codon (PTC<sup>+</sup> transcripts) in their open reading frame.<sup>15</sup> The evolutionarily-conserved post-transcriptional mechanism by which PTC<sup>+</sup> transcripts are selectively detected and degraded has been called nonsense-mediated mRNA decay (NMD).<sup>16-18</sup> This pathway acts as a quality control mechanism preventing the expression of potentially deleterious truncated proteins. Despite the fact that NMD was originally discovered in  $\beta$ -thalassemic patients and was subsequently demonstrated to be an important phenotype modulator of many human genetic diseases, including rare inherited coagulation disorders,<sup>15,19-22</sup> it is unlikely that it evolved only to protect cells against the production of truncated proteins generated by low frequency random mutations. More probably, NMD has been maintained during evolution with the primary role of degrading aberrant PTC<sup>+</sup> mRNA generated as a consequence of routine errors in gene expression such as inefficient or faulty splicing and errors introduced by RNA polymerase II.<sup>23</sup> Furthermore, it has been suggested that NMD may play a pivotal role in regulating gene expression: expression profiles of NMD-deficient yeast strains demonstrated that about 10% of the transcriptome had both qualitatively and quantitatively altered expression.<sup>24,25</sup> Likewise, comparison of expression profiles of human cells with normal or reduced NMD activity revealed that NMD targets hundreds of genes.<sup>26</sup> In this frame, it was suggested that coupling of unproductive alternative splicing and NMD might be a way to regulate gene expression post-transcriptionally,<sup>27</sup> even if it is not clear to what extent this mechanism is common within the cell.<sup>28</sup>

In this paper, we report the identification of three

novel splicing mutations causing FV deficiency. *In vitro* expression experiments were used to perform studies at the mRNA level, and the contribution of NMD in regulating the amount of a naturally skipped *F5* mRNA was investigated in HepG2 cells. In addition, we provide the first overview of alternative splicing events of the entire *F5* mRNA.

## Design and Methods

This study was approved by the Institutional Review Board of the University of Milan and was conducted according to the Declaration of Helsinki. Samples were obtained from the analyzed individuals after acquiring appropriate informed consent.

### Materials

Oligonucleotides were purchased from Sigma (St. Louis, MO, USA). Their sequences, when not reported, are available on request.

The pMT2/FV mammalian expression plasmid, containing the full-length FV complementary DNA (cDNA), was kindly provided by Dr R.J. Kaufman (Howard Hughes Medical Institute, University of Michigan Medical School, Ann Arbor, USA). Puromycin, cycloheximide, and wortmannin were purchased from Sigma and resuspended to a concentration of 1 mg/mL in water, 10 mM in dimethyl sulfoxide (DMSO), and 100 mg/mL in DMSO, respectively.

### Coagulation tests

FV activity and antigen plasma levels were measured as described elsewhere.<sup>20</sup> Briefly, the functional assay was based on the prothrombin time; FV antigen levels were determined using a sandwich enzyme immunoassay, based on a sheep anti-human polyclonal antibody (Affinity Biologicals, Hamilton, ON, Canada). In both assays, the FV level was expressed as a percentage of the level in control plasma pooled from 40 normal individuals, set as 100%. Normal ranges for FV coagulant activity (FV:C) and antigen (FV:Ag) levels were 58–140% and 64–139%, respectively. In plasma, the sensitivity of the functional and immunological tests was 1% and 0.01%, respectively.

### DNA extraction, polymerase chain reaction amplifications, and sequencing

Genomic DNA was extracted from blood samples using the Nucleon BACC1 Kit (Amersham Pharmacia Biotech, Uppsala, Sweden) and PCR-amplified under standard conditions, using sense and antisense primers designed on the basis of the known sequence of the *F5* gene (GenBank, accession number Z99572) and RED Taq DNA polymerase (Sigma). Direct sequencing of purified PCR products was performed on both strands by the fluorescent dideoxy-terminator method (BigDye Terminator Cycle Sequencing Kit, version 3.1; Applied Biosystems, Foster City, CA, USA) and analyzed using an automated multicapillary 3130 DNA sequencer (Applied Biosystems). The Variant Reporter package was used for mutation detection (Applied Biosystems).

Primers for sequencing were the same as in the amplification reactions, except those used for the 2820-bp-long exon 13, which was sequenced using additional internal primers.

### Computer-assisted splice-site prediction

Computer-assisted analysis for splice-site prediction was accomplished using the Neural Network Promoter Prediction Tool (NNPPT) program ([http://www.fruitfly.org/seq\\_tools/splice.html](http://www.fruitfly.org/seq_tools/splice.html)) and the NetGene2 (release 2.4) program (<http://www.cbs.dtu.dk/services/NetGene2>).

### Minigene construction and mutagenesis

Three *F5* regions were PCR-amplified from the genomic DNA of a healthy individual using the Expand 20 Kb<sup>PLUS</sup> PCR System (Roche Applied Science, Indianapolis, IN, USA) according to the manufacturer's instructions. Primer couples (*F5*-In6-F and *F5*-In9-R, *F5*-In19-F and *F5*-In22-R, and *F5*-In22-F and *F5*-3'UTR-R) used for these long-range amplifications are reported in Table 1. PCR products were inserted into the pTARGET vector using the pTARGET Mammalian Expression T-Vector System Kit (Promega, Milan, Italy). Plasmids were isolated using the QIAprep Spin Maxiprep Kit (Qiagen, Hilden, Germany), and the recombinant constructs, hereafter referred to as pT-*F5*(In6-In9)-wt, pT-*F5*(In20-In22)-wt, and pT-*F5*(In22-3'UTR)-wt, were checked by sequencing. The three identified mutations were introduced into the relevant wild-type construct by means of the QuickChange Site-Direct Mutagenesis Kit (Stratagene, La Jolla, CA, USA), as instructed by the manufacturer. The three mutant plasmids (namely pT-*F5*(In6-In9)-IVS8+6T>C, pT-*F5*(In20-In22)-IVS21+1G>A, and pT-*F5*(In22-3'UTR)-IVS24+1\_+4delGTAG) were checked by sequencing and extracted as described above.

The pMT2/FV plasmid was used as a template to obtain by mutagenesis a plasmid bearing the deletion (80-bp long) predicted to result from the IVS24+1\_+4delGTAG mutation. The resulting mutant plasmid (pMT2/FV-Δ80bp) was checked by sequencing and extracted as described above.

### Cell cultures, transfections, metabolic labeling, and immunoprecipitation

Human hepatoma HepG2 cells, human cervical carcinoma HeLa cells, and African green monkey kidney COS-1 cells were cultured in Dulbecco's modified Eagle's medium (DMEM), supplemented with 10% fetal bovine serum. Glutamine (1%) and antibiotics (100 IU/mL penicillin and 100 μg/mL streptomycin) were added to the medium. Cells were grown at 37°C in a humidified atmosphere of 5% CO<sub>2</sub> and 95% air and cultured according to standard procedures.

For the *in vitro* analysis of splicing products, each minigene construct was transiently transfected in HeLa cells by the calcium phosphate technique, essentially as described previously.<sup>29</sup> Recombinant FV molecules were expressed by transient transfection with the Lipofectamine 2000 reagent (Invitrogen, Carlsbad, CA, USA), as described elsewhere.<sup>30</sup> Cell lysates and conditioned media were prepared and immunoprecipitations

**Table 1.** Primers used for RT-PCR and long-range PCR.

Primer	Sequence (5'-3')	Localization	Application
<i>F5</i> -In6-F	GGACAGATGACAGAAAATGAGAAT	Intron 6	Cloning intron 6/9 fragment
<i>F5</i> -In9-R	CAGCCTCTCAGAAGTTACTAGTTGG	Intron 9	
<i>F5</i> -In19-F	ATGCCTAGACTCCTGACTACAACAC	Intron 19	Cloning intron 19/22 fragment
<i>F5</i> -In22-R	CTTTGAGTGGCAGTGAGAAAATAAT	Intron 22	
<i>F5</i> -In22-F	GTGGCTGTGTACCTTAGACAAGIT	Intron 22	Cloning intron 22/3'UTR fragment
<i>F5</i> -3'UTR-R	CTAATGACCACCAACCTTGAATATC	3' UTR	
RT-7-F	GAGGCGGCACATGAAGAG	Exon 7	RT-PCR analysis of pT- <i>F5</i> (In6-In9) construct
RT-9-R	GGCGAGAAGGTCACCTCCA	Exon 9	
RT-20-F	GGGAGCCCAGATTAGCAAG	Exon 20	RT-PCR analysis of pT- <i>F5</i> (In20-In22) construct
RT-22-R	TTGCAGTTCCAATCGAAGG	Exon 22	
RT-23-F	CACCCCTGGGTATGGAAA	Exon 23	RT-PCR analysis of pT- <i>F5</i> (In6-In9) construct
RT-25-R	GAGTCCAGCGAAGTGC	Exon 25	
<i>F5</i> -ex2/4-F	ATTCAG/GTGCTTCTTACCTTGAC	Exon 2/4 junction	Detection of Δ3 transcript
<i>F5</i> -ex5-R	TGGGAGTAAATAGATGTGTGTGAGG	Exon 5	
<i>F5</i> -ex4/7-F	TATCTGTAAAAAG/CTGGGATGC	Exon 4/7 junction	Detection of Δ5-6 transcript
<i>F5</i> -ex8-R	TTCACTGTATGTTTGGTGAAGGA	Exon 8	
<i>F5</i> -ex7/9-F	AGCGAATATGGACAA/ATCGTG	Exon 7/9 junction	Detection of Δ8 transcript
<i>F5</i> -ex11-R	CTCATCAAAACACAGCAACACA	Exon 11	
<i>F5</i> -ex7/8-F	CCAGCGAATATGGACAA/AAAAT	Exon 7/8 junction	Real-time PCR analysis of alternative transcript degradation
<i>F5</i> -ex8-R	TTCACTGTATGTTTGGTGAAGGA	Exon 8	
<i>F5</i> -ex7/9-F	AGCGAATATGGACAA/ATCGTG	Exon 7/9 junction	Real-time PCR analysis of alternative transcript degradation
<i>F5</i> -ex9-R	CCTGCCTGAGGTGAAGAAG	Exon 9	

The symbol "/" within the primer sequence indicates the position of the exon-exon junction.

carried out as described by Duga *et al.*<sup>30</sup> The immunoprecipitated proteins were resolved by 6% sodium dodecyl sulphate-polyacrylamide gel electrophoresis (SDS-PAGE) under non-reducing conditions. Gels were dried under vacuum at 80°C for 1 hour. The labeled proteins were visualized by exposing gels overnight to a storage phosphor screen (Amersham Pharmacia Biotech) and analyzed using a Typhoon 9200 phosphor imager (Amersham Pharmacia Biotech).

### Inhibition of the NMD pathway

HepG2 cells were plated at a density of 5.5×10<sup>6</sup> per 10-cm dish and, after 72 hours, treated with three inhibitors of NMD (puromycin, cycloheximide, and wortmannin): puromycin and cycloheximide block NMD by interfering with protein synthesis, whereas wortmannin selectively inhibits phosphatidylinositol 3-kinase (PI3K), a kinase that is able to phosphorylate PI-3-kinase-related kinase SMG-1 (SMG1) which, in turn, phosphorylates up-frameshift suppressor 1 (Upf1), a regulator of non-

**Table 2. Clinical and genetic characteristics of the FV-deficient patients analyzed.**

Clinical data				
Patient	A	B	C	
Sex	F	M	F	
Age at diagnosis	n.a.	54	31	
Origin	Iran	Italy	Austria	
Consanguinity	Yes <sup>a</sup>	No	No <sup>a</sup>	
Main symptoms	Epistaxis	Intracranial bleeding due to severe hypertension	Bleedings: muscle, gastrointestinal, urogenital, spleen	
FV:C (%) <sup>b</sup>	5%	<1%	3%	
FV:Ag (%) <sup>c</sup>	6%	0.1%	n.a.	
Genetic data				
Patient	Status	Genomic <sup>d</sup>	cDNA <sup>e</sup>	Mature protein <sup>f</sup>
A	Homozygous	IVS8+6T>C	-	p.Lys346SerfsX17
B	Compound heterozygous	IVS21+1G>A g.51452C>T	- c.3178C>T	p.Gly1952ValfsX2 Arg1002ter
C	Compound heterozygous	IVS24+1_+4delGTAG g.75002G>A	- c.6395G>A	p.Met2120IlefsX12 Arg2074His

<sup>a</sup>Unknown degree of consanguinity. <sup>b</sup>Normal range: 58% to 140%. <sup>c</sup>Normal range: 64% to 139%. <sup>d</sup>Numbering according to GenBank, accession number Z99572, inverted and complemented. <sup>e</sup>Numbering according to GenBank, accession number M16967. <sup>f</sup>Consequences at the protein level of splicing mutations were either predicted or demonstrated by in vitro experiments. n.a.: not available.

sense transcripts which plays a pivotal role in NMD. Puromycin, used at the concentration of 100 µg/mL, was applied to cells for 8 hours, whereas both cycloheximide (100 µg/mL) and wortmannin (20 µM) were applied to cells for 4 hours.

After the treatment, cells were washed twice with PBS and total RNA was extracted as described below. Non-treated samples were incubated with the corresponding drug solvent.

### RNA extraction and reverse transcriptase-polymerase chain reaction

Total RNA was isolated from platelets, HeLa, and HepG2 cells using the RNeasyWIZ reagent (Ambion, Austin, TX, USA). Liver RNA was extracted by the acid guanidinium thiocyanate-phenol-chloroform method described by Chomczynski and Sacchi.<sup>31</sup> Random non-amers and the Enhanced Avian RT-PCR Kit (Sigma) were used to perform first-strand cDNA synthesis starting from 1.5 µg of total RNA, according to the manufacturer's instructions. Of a total 20-µL mixture, 1-2.5 µL were used as a template to amplify wild-type and mutant transcripts, using exonic primer couples (Table 1). PCR were carried out using RED *Taq* DNA polymerase under standard conditions.

### Real-time RT-PCR

Real-time PCR assays were performed using the iQ5 real-time PCR detection system (Biorad, Hercules, CA, USA) and the iQ SYBER Green Supermix kit (Biorad) according to the manufacturer's instructions. In each reaction, 1.5 µL of cDNA from treated or untreated

HepG2 cells were used. Differences in *F5*-Δ8-mRNA abundance were quantified by the ΔΔCT method.<sup>32</sup> The *F5* wild-type transcript was used as the reference. Primer couples, designed to specifically amplify *F5* transcripts including or not exon 8, are listed in Table 1.

## Results

### Case reports and laboratory analysis

Three unrelated patients (A, B, and C) affected by FV deficiency were analyzed (Table 2). Patient A is an Iranian woman, born from a consanguineous marriage. Her FV plasma levels were moderately reduced (FV:C=5% and FV:Ag=6%); she suffered only from epistaxis and was successfully treated with fresh-frozen plasma. Her siblings did not report any bleeding problems.

Patient B was an Italian man from Sassari (Sardinia). At the time of blood sampling he was 54 years old; he died 2 years later from intracranial bleeding due to severe hypertension. No FV activity could be detected in his plasma (<1%), and his FV antigen level was severely reduced (0.1%).

Patient C is a 31-year old woman from Austria, whose FV:C levels were reduced to 3%. She suffered from repeated bleeding, without preceding trauma; she had had frequent nosebleeds (starting at the age of 13 months and ceasing at the age of 7 years), had repeated muscle hemorrhages in the lower limbs, a gastrointestinal hemorrhage (at the age of 10 years), and macrohematuria. She also presented with spleen rupture, treated with splenectomy. None of her relatives was reported to have bleeding problems.

### Mutational screening

The whole coding region, all intron-exon boundaries, and about 300 bp of the promoter region of the *F5* gene were PCR-amplified from the patients' genomic DNA. Direct sequencing of all amplified fragments allowed us to identify five genetic defects, three of which were hitherto unknown (IVS8+6T>C, IVS21+1G>A, and IVS24+1\_+4delGTAG) while the other two had been previously described [g.75002G>A, leading to the Arg2074His missense substitution,<sup>33</sup> and g.51452C>T, causing the Arg1002ter nonsense mutation]<sup>34</sup> (Table 2). IVS8+6T>C was the only mutation found in the homozygous state in patient A, while patients B and C were compound heterozygotes for the IVS21+1G>A and Arg1002ter, and for the IVS24+1\_+4delGTAG and Arg2074His mutations, respectively. The two already described genetic defects were not further investigated, whereas the three putative splicing mutations, whose absence in the general population was verified by sequencing 200 haploid genomes, were characterized in depth.

### Splice-site predictions

The effect of the predicted splicing mutations (IVS8+6T>C, IVS21+1G>A, and IVS24+1\_+4delGTAG) was first analyzed by computer-assisted splice-site prediction using the NNPT and NetGene 2 programs. As far as the IVS8+6T>C mutation is concerned, both pro-

grams recognized the wild-type as well as the mutant splice site without any appreciable score reduction (0.98 vs. 0.99 and 0.94 vs. 0.90 for the NNPT and NetGene2, respectively). Conversely, no donor splice site was identified, either in the wild-type or in the mutant sequence, in the region surrounding the IVS21+1G>A mutation. Finally, this *in silico* analysis detected the wild-type donor splice site of exon 24 with a score of 0.68 using the NNPT and of 0.92 with NetGene2, whereas the mutant sequence was no longer identified as a donor splice site.

**Production of F5 mRNA in HeLa cells**

To examine the effects of the IVS8+6T>C, IVS21+1G>A, and IVS24+1\_+4delGTAG mutations on F5 pre-mRNA splicing, appropriate F5 minigene constructs (namely pT-F5(In6-In9)-wt, pT-F5(In20-In22)-wt and pT-F5(In22-3'UTR)-wt) were generated, by cloning the relevant PCR-amplified genomic fragment into the mammalian expression vector pTARGET (Figure 1A, B,

C left panels). The orientation of the inserts and absence of unanticipated changes due to PCR errors in the cloned regions were checked by sequencing. Subsequently, these three vectors were subjected to site-directed mutagenesis to obtain recombinant constructs containing the identified defects.

Wild-type and mutant plasmids were independently transfected in HeLa cells (not expressing FV). Total RNA was extracted after 48 hours and RT-PCR assays were performed to analyze the splicing pattern of both wild-type and mutant transcripts (Figure 1): all mutant minigene constructs gave rise to fragments with different electrophoretic mobility compared to that of the wild-type ones. In particular, the RT-PCR product derived from the IVS8+6T>C mutant vector was approximately 180 bp shorter than the wild-type one, and direct sequencing of this fragment demonstrated that the entire exon 8 was skipped from the mature mRNA (Figure 1A middle and right panels). RT-PCR analyses

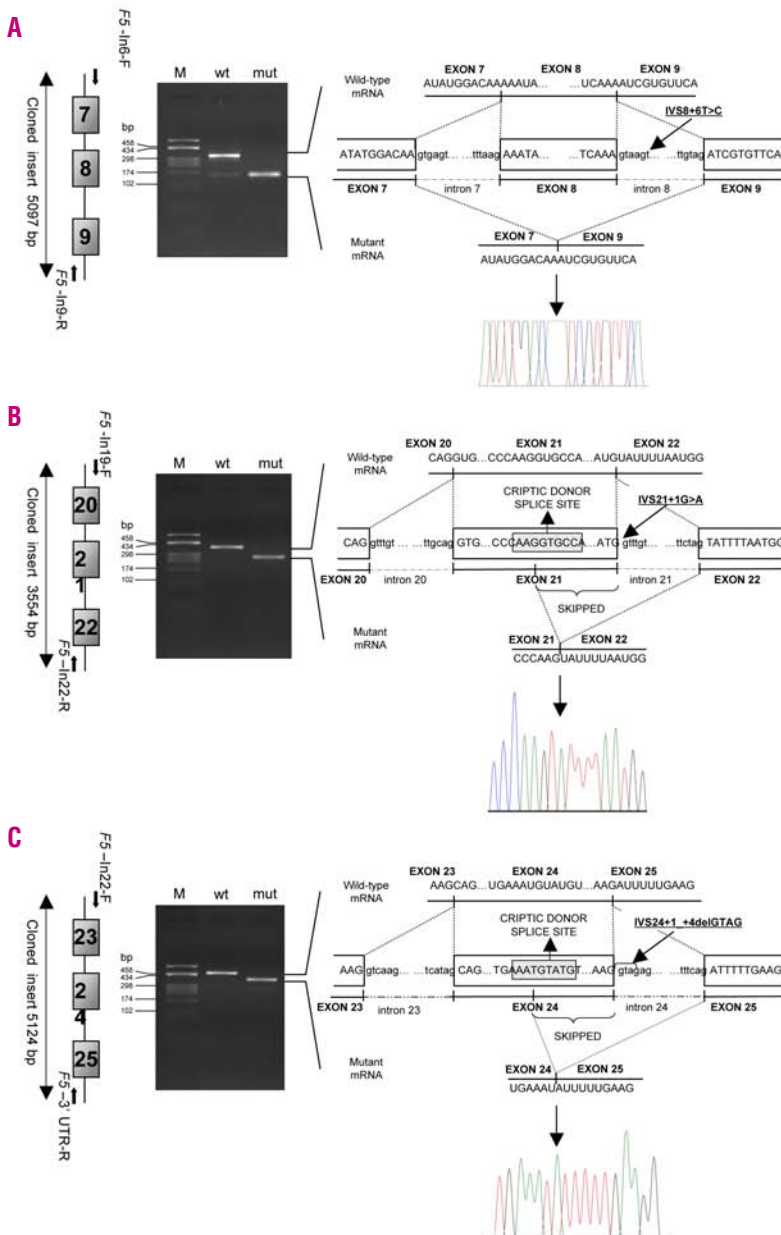


**Figure 1.** Functional analysis of the effect of IVS8+6T>C, IVS21+1G>A, and IVS24+1\_+4 delGTAG mutations on F5 pre-mRNA splicing. (A,B,C) Left panels: Schematic representation of the F5 regions cloned to produce minigene constructs. Exons (numbered) are indicated by boxes, introns are represented by lines and are not to scale. Primers used in cloning experiments are indicated by arrows showing the primer orientation. Middle panels: RT-PCR products obtained from RNA of cells transfected with the relevant minigene construct, separated on a 2% agarose gel (primer couples are listed in Table 1). Lane M: molecular weight marker (pUC98-HaeIII); lanes 1 and 2: RT-PCR products amplified from transfected HeLa cells expressing wild-type and mutant constructs, respectively. Right panels: schematic representation of normal (above) and aberrant (below) splicing events. The three mutations identified are indicated by arrows. In the panels in B and C the cryptic donor splice sites activated by the mutations are shaded in gray and the skipped portions of exons 21 and 24 are indicated by a curly bracket.

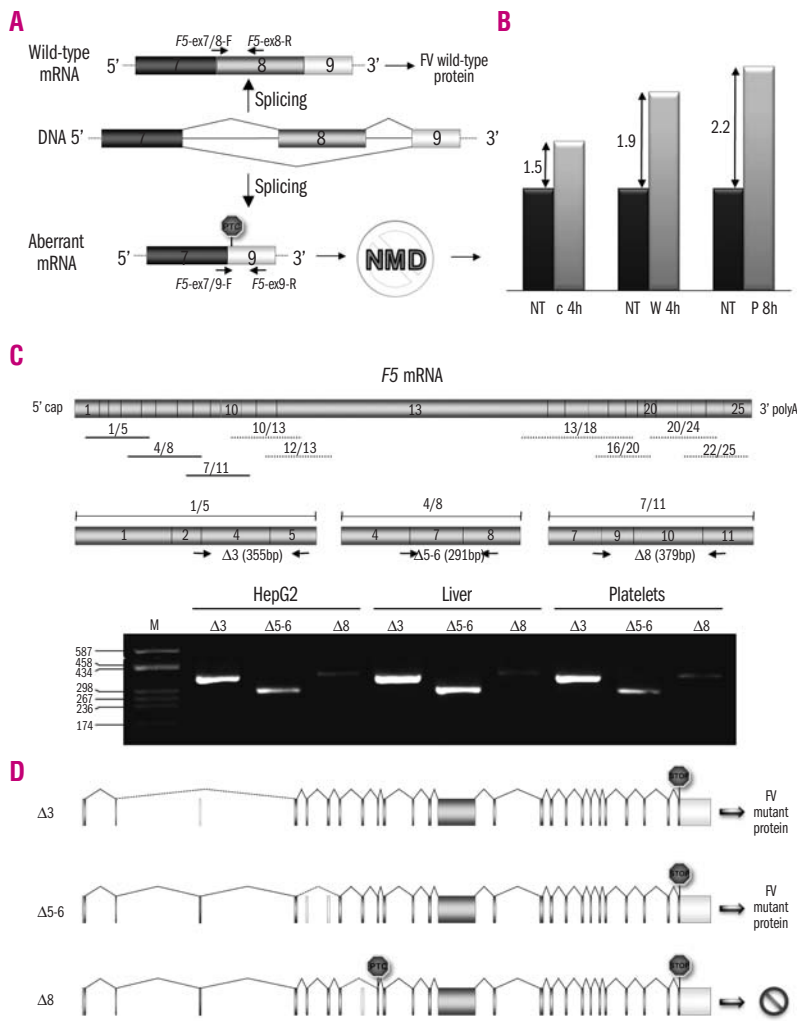


**Figure 2.** Analysis of *F5* alternative splicing pattern. **(A)** Schematic representation of the *F5* gene exon-intron structure between exons 7 and 9 and of the predicted destiny of normal (above) and aberrant (below) *F5* mRNA. Exons (numbered) are indicated by boxes, introns (not to scale) are indicated by lines. The positions of the primer couples used to amplify the wild-type (*F5*-Ex7/8-F and *F5*-Ex8-R) as well as the  $\Delta 8$  transcripts (*F5*-Ex7/9-F and *F5*-Ex9-R) are indicated. **(B)** Effect of NMD inhibition on *F5*  $\Delta 8$  transcript levels. Real-time RT-PCR assays were used to quantify the increase of  $\Delta 8$  mRNA after treatment of HepG2 cells with the NMD inhibitors cycloheximide (C 4h), wortmannin (W 4h), and puromycin (P 8h). The *F5* wt transcript (*i.e.* containing exon 8) was used as the reference. In each experiment, untreated samples were used as calibrators. The fold-increases of skipped *F5* mRNA due to the treatments are graphically represented by arrows. **(C)** Top: Schematic representation of the *F5* mRNA showing the position of the 24 exon-exon junctions. The overlapping fragments amplified to analyze the *F5* splicing pattern are indicated by lines, continuous lines representing amplicons that highlighted the presence of an alternative splicing event. The numbers above the lines indicate the spanned exons. Middle: enlargement of RT-PCR fragments spanning exons 1/5, 4/8, and 7/11. The position of primer couples designed to specifically amplify alternative *F5* transcripts, as well as the sizes of expected PCR products are indicated. Bottom: RT-PCR products amplified from total RNA extracted from HepG2 cells, liver, and platelets separated on a 2% agarose gel. Lane M: molecular weight marker (*pUC9-HaeIII*), lane  $\Delta 3$ ,  $\Delta 5-6$ , and  $\Delta 8$ : RT-PCR products resulting from the amplification of alternative *F5* mRNA lacking exons 3, 5-6, and 8, respectively. **(D)** Schematic representation of the three identified alternative *F5* transcripts. Exons (boxes) and introns (lines) are drawn to scale. Splicing events are shown by broken continuous and hatched lines (constitutive and alternative splicing, respectively). Skipped exons are in light gray.

demonstrated that transcripts produced from the IVS21+1G>A and IVS24+1\_+4delGTAG mutant plasmids (approximately 100 and 80 bp shorter than the wild-type ones) were generated by the use of cryptic donor splice sites located in exons 21 and 24, respectively (Figure 1B and C, middle and right panels). In all cases, the splicing defect would result in the introduction of a PTC. It has been demonstrated that PTC located within a distance of 50-55 nucleotides from the last exon-exon junction or located in the last exon fail to trigger this surveillance system.<sup>12</sup> Based on this rule, PTC<sup>+</sup> mRNA resulting from the IVS8+6T>C and IVS21+1G>A mutations are probably subjected to NMD and consequently will not be translated into a mutant protein, whereas the PTC<sup>+</sup> transcript resulting from the IVS24+1\_+4delGTAG mutation is supposed not to be detected and degraded by NMD, thus leading to the synthesis of a truncated FV protein (p.Met2120IlefsX12; numbering omits the signal peptide).

**Expression of wild-type and mutant recombinant FV in COS-1 cells**

The effect of the IVS24+1\_+4delGTAG mutation on FV secretion was investigated by *in vitro* expression of

mutant and wild-type FV molecules in COS-1 cells, which do not express endogenous FV. To this purpose, the pMT2/FV expression plasmid, containing the full-length *F5* cDNA, was subjected to mutagenesis, to remove the same 80 nucleotides skipped in the IVS24+1\_+4delGTAG mutant transcript. Cells were independently transfected with either the wild-type or the mutant plasmid. After labeling with [<sup>35</sup>S]-methionine and [<sup>35</sup>S]-cysteine for 16 hours, recombinant FV molecules were collected by immunoprecipitation from culture media and cell lysates. As for the wild-type protein, SDS-PAGE showed normal secretion of the molecule; by contrast, the mutant FV was detectable only intracellularly (*data not shown*).

**Analysis of the F5 splicing pattern**

Interestingly, RT-PCR analysis of the effect of the IVS8+6T>C mutation on splicing showed that a PCR fragment with the same electrophoretic mobility as that of the mutant one was also detectable in cells producing the wild-type transcript (Figure 1A middle panel, lane *w*). To verify the hypothesis of the existence of alternative physiological splicing, skipping the entire exon 8 (Figure 2A), total RNA extracted from human liver, platelets, and

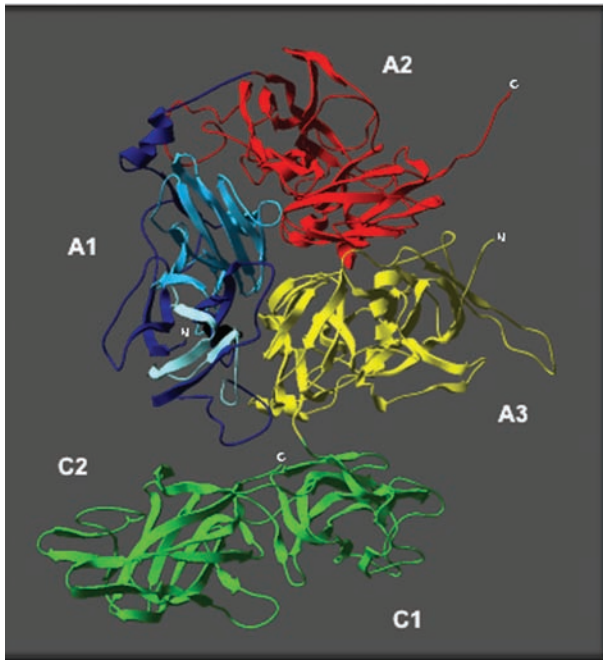


**Figure 3.** Three-dimensional model of human FVa showing the protein regions removed by exon 3 and exon 5-6 in-frame skipping. Ribbon diagram of human FVa, produced using SwissPDB 3.7 software and the coordinates deposited under Protein Data Bank entry 1FV4. The three A domains of FV are shown in blue (A1), red (A2), and yellow (A3), whereas the two C domains are shown in green. The model is oriented to best display the amino acid regions encoded by *F5* exon 3 (41 residues) and exons 5-6 (122 residues), which are colored with different shades of light blue. N and C indicate the amino- and carboxy-termini of the heavy and light chains.

HepG2 cells (normally producing FV) was subjected to RT-PCR analysis. For this analysis, a specific primer couple was designed to amplify only the aberrant mRNA (Table 1). RT-PCR analysis demonstrated that exon-8 skipping took place physiologically in all the samples analyzed (Figure 2C).

Since skipping of the entire exon 8 leads to the generation of a PTC, and considering that it was previously demonstrated that *F5* is a target of the NMD pathway (at least in pathological conditions, *i.e.* in FV-deficient patients with truncating mutations),<sup>20,21</sup> we decided to investigate whether the *physiological* exon-8-skipped mRNA (henceforth called *F5-Δ8*-mRNA) is also degraded by this mRNA surveillance system. For this purpose, wortmannin, cycloheximide, and puromycin were used to inhibit NMD in HepG2 cells, in order to upregulate the expression of those transcripts that normally undergo NMD degradation. Total RNA was extracted from treated and untreated HepG2 cells and the relative quantity of *F5-Δ8*-mRNA was assessed by real-time RT-PCR. This analysis demonstrated an increase in the expression of the *F5-Δ8*-mRNA in treated cells. In particular, wortmannin induced a 1.9-, cycloheximide a 1.5- and puromycin a 2.2-fold increase (Figure 2B), confirming that *F5-Δ8*-mRNA is downregulated by NMD.

These results prompted us to analyze the *F5* splicing pattern further using total RNA isolated from HepG2 cells treated with puromycin. A set of RT-PCR assays was designed to pick up the vast majority of possible alterna-

tive splicing events (Figure 2C). The most interesting results were obtained with RT-PCR assays covering the 5' region of the *F5* mRNA, where three major alternative splice events were detected (*data not shown*). Their lengths, on the basis of electrophoretic mobility, were compatible with skipping of exons 3, 5-6, and 8 (as expected). To confirm these predicted skipping events, RT-PCR assays were performed using specific primer couples (Table 1) on human liver, platelet, and HepG2 RNA; the fragments obtained were also subjected to direct sequencing, demonstrating the physiological expression of  $\Delta 3$ ,  $\Delta 8$ , and  $\Delta 5-6$  transcripts in the tissues analyzed (Figure 2C, D). Given that exon 3 and exon 5-6 skipping are in frame, the resulting mRNA do not contain a PTC and are predicted to cause the synthesis of a FV protein lacking 41 (for  $\Delta 3$ ) and 122 (for  $\Delta 5-6$ ) amino acids in the A1 domain. As shown in Figure 3, the 41 amino acids encoded by exon 3 form three  $\beta$ -strands involved in the formation of the N-terminal  $\beta$ -sandwich of the domain, whereas the removal of the 122 amino acids caused by exon 5-6 skipping affects almost the whole C-terminal  $\beta$ -sandwich. The 122-residue deletion is also predicted to abolish the disulfide bridge between Cys220 and Cys301, which is involved in stabilizing the entire A1 domain.

## Discussion

In this work, we studied three unrelated patients with FV deficiency. Laboratory data from blood samples from these three individuals showed reduced FV antigen levels and coagulant activity. The clinical symptoms of all the patients concurred well with the bleeding pattern reported in the literature.<sup>3</sup>

Among rare inherited bleeding disorders, FV deficiency is one of the least characterized from the molecular point of view, with only 42 genetic defects hitherto described.<sup>1,6,11</sup> Most of the genetic abnormalities are nonsense, frameshift or missense mutations, whereas, up to now, only four splicing defects have been fully described.

To unravel the molecular basis of FV deficiency in our patients, we performed a complete mutational screening of the *F5* gene, which revealed five point mutations. Two of these mutations (Arg2074His and Arg1002ter) have already been described<sup>1,33,34</sup> and were not analyzed further. The remaining three novel defects (IVS8+6T>C, IVS21+1A>G and IVS24+1\_+4delGTAG), all located in donor splice sites, were investigated in depth.

Up to 10% of all point mutations causing human genetic diseases result in an mRNA splicing defect [HGMD, Human Gene Mutation Database, <http://www.hgmd.cf.ac.uk/ac/index.php>].<sup>35</sup> In the majority of cases, splicing mutations cause the disruption of a pre-existing splice site, frequently resulting in exon skipping.<sup>36</sup> The opposite situation, *i.e.* the activation of a cryptic splice site by point mutation, is less frequent.<sup>37</sup> The *F5* splicing mutations so far described are located in intron-8 acceptor [IVS8-2A>G],<sup>14</sup> exon-10 donor [1701G>T]<sup>12</sup>, intron-16 acceptor [IVS16-3G>T],<sup>10</sup> and intron-19 donor [IVS19+3A>T]<sup>13</sup> splice sites. The IVS16-3G>T mutation was not investigated at the mRNA level (at least as far as can be deduced from reading the English abstract, since the paper is in

Chinese) whereas, in the remaining cases, the mutations cause the disruption of the canonical splice sites, leading either to the activation of a cryptic splice site<sup>12,14</sup> or to complete exon skipping.<sup>13</sup> The only mutation introducing a PTC is the 1701G>T; in fact, both IVS8-2A>G and IVS19+3A>T generate an in-frame transcript coding for a FV mutant protein, with an addition of eight amino acids in the A2 domain and a partial deletion of the C2 domain, respectively.

To predict the possible effect of the newly identified mutations on *F5* pre-mRNA splicing, computer-assisted splice-site prediction analysis was performed with two programs available online. These tools recognized a significant difference between the wild-type and the mutant sequence only for IVS24+1\_+4delGTAG. Since *in silico* analyses were partially inconclusive, and considering the impossibility of obtaining biological specimens suitable for RNA extraction from either the patients or their relatives, we decided to study the effects of the identified mutations on *F5* splicing using an *in vitro* approach. This analysis demonstrated that all the splicing mutations inactivate the corresponding donor splice site. In the case of IVS8+6T>C the entire exon 8 is skipped from mature mRNA, whereas IVS21+1G>A and IVS24+1\_+4delGTAG both activate a cryptic donor splice site (located in exons 21 and 24, respectively). In all cases, the splicing defect would determine the introduction of a PTC, 1833, 242, and 64 residues before the canonical stop. Considering that it was previously demonstrated that the *F5* gene is subjected to NMD,<sup>20,21</sup> only mRNA carrying the IVS8+6T>C and IVS21+1G>A mutations are predicted to be degraded by this pathway, their PTC being located before the last exon of *F5*. In contrast, the IVS24+1\_+4delGTAG splicing defect leads to the introduction of a PTC in the last exon of the gene, thus determining the synthesis of a truncated FV protein, whose fate was investigated by *in vitro* expression experiments. This analysis demonstrated that the FV mutant molecule was not competent for secretion, as expected for FV molecules with partial deletion of the C2 domain.<sup>13,38,39</sup> These results clearly demonstrated the causal role of each of the identified mutations in determining FV deficiency.

Interestingly, the molecular characterization of IVS8+6T>C led to the identification of physiological alternative splicing involving skipping of exon 8. The presence of this naturally occurring alternative splicing was confirmed in HepG2 cells, human liver, and platelets. Since exon-8 skipping leads to the generation of a PTC, we decided to investigate whether this *F5*- $\Delta$ 8-mRNA is indeed degraded by NMD. For this purpose, three inhibitors of NMD were used to treat HepG2 cells and real-time RT-PCR assays were performed to evaluate the possible increase in the aberrant mRNA level in treated *vs.* untreated samples: in all cases an increase was detected in the expression of the *F5*- $\Delta$ 8-mRNA. This finding is interesting considering that the action of NMD on *F5* transcripts has, up to now, been evaluated only in the case of PTC<sup>+</sup> mRNA determined by FV-deficiency-causing mutations<sup>20,21</sup> but has never been evaluated on physiologically alternatively spliced transcripts. Furthermore, the identi-

cation of the first *F5* alternative splicing event associated with NMD suggests that *F5* gene expression could be regulated post-transcriptionally by a mechanism coupling alternative splicing and NMD.<sup>27,28</sup>

To analyze the *F5* splicing pattern further, RT-PCR assays covering almost the whole *F5* coding sequence were performed. This analysis revealed the occurrence of multiple alternative splicing events; among the various fragments produced, we further characterized the *major* ones, which, on the basis of their electrophoretic mobility, showed in-frame exon skipping (*i.e.* exons 3 and 5-6). The presence of these alternative splices was confirmed in human liver and platelets by specific RT-PCR assays followed by direct sequencing of the amplified fragments. Interestingly, for all three naturally occurring alternative splicing events, *in silico* splice-site prediction analysis of the exons involved in the skipping events revealed that either the acceptor or the donor wild-type splice site was not identifiable, suggesting that the observed *aberrant* skipping could possibly be related to the weakness of such sites. The predicted FV molecules translated from the *F5*  $\Delta$ 3 and the  $\Delta$ 5-6 transcripts would lack 41 and 122 amino acids, respectively, in the A1 domain. It can be hypothesized that such drastic deletions would perturb packing of the A1 domain, likely affecting protein stability and competence for secretion, as demonstrated for other recombinant FV mutant proteins.<sup>13,38,39</sup> Should these proteins be secreted into the circulation, it is conceivable that they would be expressed at extremely low levels, as demonstrated by the very low levels of the transcripts detected in HepG2 cells (*data not shown*).

In conclusion, we have demonstrated the functional consequences of three novel splicing mutations leading to FV deficiency. Furthermore, the comprehensive analysis of the *F5* splicing pattern led to the identification of two in-frame splicing variants and one out-of-frame alternative splicing event, which was demonstrated to be downregulated by the NMD pathway, thus suggesting a possible role of a mechanism coupling alternative splicing and NMD in the regulation of *F5* expression.

---

## Authorship and Disclosures

All the authors participated in the conception and design of the present study, in the analysis and interpretation of the data, and in revising the manuscript. CDO, IG, NL, EMP, and MS were responsible for PCR amplifications, sequence analysis, site-directed mutagenesis, expression experiments, and drafting the manuscript. SD participated in the conception of the study, interpretation of the results, and in reviewing the manuscript. MLT was involved in the study design and in the discussion of the results. AA, CP, and FP were responsible for the recruitment and clinical management of the patients. RA participated in writing the manuscript and supervised the entire study. The authors reported no potential conflicts of interest.

## References

- Asselta R, Tenchini ML, Duga S. Inherited defects of coagulation factor V: the hemorrhagic side. *J Thromb Haemost* 2006;4:26-34.
- Mannucci PM, Duga S, Peyvandi F. Recessively inherited coagulation disorders. *Blood* 2004;104:1243-52.
- Lak M, Sharifian R, Peyvandi F, Mannucci PM: Symptoms of inherited factor V deficiency in 35 Iranian patients. *Br J Haematol* 1998;103:1067-9.
- Kent WJ, Sugnet CW, Furey TS, Roskin KM, Pringle TH, Zahler AM, et al. The Human Genome Browser at UCSC. *Genome Res* 2002;12:996-1006.
- Cripe LD, Moore KD, Kane WH. Structure of the gene for human coagulation factor V. *Biochemistry* 1992;31:3777-85.
- Kling SJ, Griffie M, Flanders MM, Rodgers GM. Factor V deficiency caused by a novel missense mutation, Ile417Thr, in the A2 domain. *J Thromb Haemost* 2006;4:481-3.
- Yamakage N, Ikejiri M, Okumura K, Takagi A, Murate T, Matushita T, et al. A case of coagulation factor V deficiency caused by compound heterozygous mutations in the factor V gene. *Haemophilia* 2006;12:172-8.
- Asselta R, Dall'Osso C, Duga S, Spreafico M, Saxena R, Tenchini ML. Coagulation factor V gene analysis in five Indian patients: identification of three novel small deletions. *Haematologica* 2006;91:1724-6.
- Jones CD, Yeung C, Negro F, Zehnder JL. Molecular characterization and subcellular localization of Tyr478del: a pathogenic in-frame deletion in coagulation factor V. *J Thromb Haemost* 2007;5:431-3.
- Zheng WD, Liu YH, Liu HF, Chen ZH, Wang Y. Identification of two novel mutations of human blood coagulation factor V gene in a Chinese family with congenital factor V deficiency. *Zhonghua Yi Xue Yi Chuan Xue Za Zhi* 2006;5:515-8.
- Caudill JS, Sood R, Zehnder JL, Pruthi RK, Steensma DP. Severe coagulation factor V deficiency associated with an interstitial deletion of chromosome 1q. *J Thromb Haemost* 2007;5:626-8.
- Schrijver I, Koerper MA, Jones CD, Zehnder JL. Homozygous factor V splice site mutation associated with severe factor V deficiency. *Blood* 2002;99:3063-5.
- Asselta R, Montefusco MC, Duga S, Malcovati M, Peyvandi F, Mannucci PM, et al. Severe factor V deficiency: exon skipping in the factor V gene causing a partial deletion of the C1 domain. *J Thromb. Haemost* 2003;1:1237-44.
- Fu QH, Zhou RF, Liu LG, Wang WB, Wu WM, Ding QL, et al. Identification of three F5 gene mutations associated with inherited coagulation factor V deficiency in two Chinese pedigrees. *Haemophilia* 2004;10:264-70.
- Frischmeyer PA, Dietz HC. Nonsense-mediated mRNA decay in health and disease. *Hum Mol Genet* 1999;10:1893-900.
- Losson R, Lacroute F. Interference of nonsense mutations with eukaryotic messenger RNA stability. *Proc Natl Acad Sci USA* 1979;76:5134-7.
- Maquat LE. Nonsense-mediated mRNA decay: splicing, translation and mRNP dynamics. *Nat Rev Mol Cell Biol* 2004;5:89-99.
- Lejeune F, Maquat LE. Mechanistic links between nonsense-mediated mRNA decay and pre-mRNA splicing in mammalian cells. *Curr Opin Cell Biol* 2005;17:309-15.
- Holbrook JA, Neu-Yilik G, Hentze MW, Kulozik AE. Nonsense-mediated decay approaches the clinic. *Nat Genet* 2004;36:801-8.
- Montefusco MC, Duga S, Asselta R, Santagostino E, Mancuso G, Malcovati M, et al. A novel two base pair deletion in the factor V gene associated with severe factor V deficiency. *Br J Haematol* 2000;111:1240-6.
- van Wijk R, Montefusco MC, Duga S, Asselta R, van Solinge W, Malcovati M, et al. Coexistence of a novel homozygous nonsense mutation in exon 13 of the factor V gene with the homozygous Leiden mutation in two unrelated patients with severe factor V deficiency. *Br J Haematol* 2001;114:871-4.
- Soldà G, Asselta R, Ghiotto R, Tenchini ML, Castaman G, Duga S. A type II mutation (Glu117stop), induction of allele-specific mRNA degradation and factor XI deficiency. *Haematologica* 2005;90:1716-8.
- Maquat LE. Nonsense-mediated mRNA decay in mammals. *J Cell Sci* 2005;118:1773-6.
- He F, Li X, Patrick P, Casillo R, Dong S, Jacobson A. Genome-wide analysis of mRNAs regulated by the nonsense-mediated and 5' to 3' mRNA decay pathways in yeast. *Mol Cell* 2003;12:1439-52.
- Lelivelt MJ, Culbertson MR. Yeast Upr proteins required for RNA surveillance affect global expression of the yeast transcriptome. *Mol Cell Biol* 1999;19:6710-9.
- Mendell JT, Sharifi NA, Meyers JL, Martinez-Murillo F, Dietz HC. Nonsense surveillance regulates expression of diverse classes of mammalian transcripts and mutates genomic noise. *Nat Genet* 2004;36:1073-8.
- Green RE, Lewis BP, Hillman RT, Blanchette M, Lareau LF, Garnett AT, et al. Widespread predicted nonsense-mediated mRNA decay of alternatively-spliced transcripts of human normal and disease genes. *Bioinformatics* 2003;19:118-21.
- Pan Q, Saltzman AL, Kim YK, Misquitta C, Shai O, Maquat LE, et al. Quantitative microarray profiling provides evidence against widespread coupling of alternative splicing with nonsense-mediated mRNA decay to control gene expression. *Genes Dev* 2006;20:153-8.
- Asselta R, Duga S, Simonic T, Malcovati M, Santagostino E, Giangrande PL, et al. Afibrinogenemia: first identification of a splicing mutation in the fibrinogen  $\gamma$  chain gene leading to a major  $\gamma$  chain truncation. *Blood* 2000;96:2496-500.
- Duga S, Montefusco MC, Asselta R, Malcovati M, Peyvandi F, Santagostino E, et al. Arg2074Cys missense mutation in the C2 domain of factor V causing moderately severe factor V deficiency: molecular characterization by expression of the recombinant protein. *Blood* 2003;101:173-7.
- Chomczynski P, Sacchi N. Single-step method of RNA isolation by acid guanidiniumthiocyanate phenolchloroform extraction. *Anal Biochem* 1987;162:156-9.
- Livak KJ, Schmittgen TD. Analysis of relative gene expression data using real-time quantitative PCR and the  $2^{-\Delta\Delta Ct}$  method. *Methods* 2001;25:402-8.
- Schrijver I, Houissa-Kastally R, Jones CD, Garcia KC, Zehnder JL. Novel factor V C2-domain mutation (R2074H) in two families with factor V deficiency and bleeding. *Thromb Haemost* 2002;87:294-9.
- Montefusco MC, Duga S, Asselta R, Malcovati M, Peyvandi F, Santagostino E, et al. Clinical and molecular characterization of 6 patients affected by severe deficiency of coagulation factor V: broadening of the mutational spectrum of factor V gene and in vitro analysis of the newly identified missense mutations. *Blood* 2003;102:3210-6.
- Krawczak M, Cooper DN. The human gene mutation database. *Trends Genet* 1997;13:121-2.
- Krawczak M, Reiss J, Cooper DN. The mutational spectrum of single base-pair substitutions in mRNA splice junctions of human genes: causes and consequences. *Hum Genet* 1992;90:41-54.
- Talerico M, Berget SM. Effect of 5' splice site mutations on splicing of the preceding intron. *Mol Cell Biol* 1990;12:6299-305.
- Ortel TL, Devore-Carter D, Quinn-Allen M, Kane WH. Deletion analysis of recombinant human factor V. Evidence for a phosphatidylserine binding site in the second C-type domain. *J Biol Chem* 1992;267:4189-98.
- Zhang JX, Braakman I, Matlack KE, Helenius A. Quality control in the secretory pathway: the role of calreticulin, calnexin and BiP in the retention of glycoproteins with C-terminal truncations. *Mol Biol Cell* 1997;8:1943-54.
- Shapiro MB, Senapathy P. RNA splice junctions of different classes of eukaryotes: sequence statistic and functional implications in gene expression. *Nucleic Acids Res* 1987;15:7155-74.